Decoding the principles underlying the frequency of association with nucleoli for RNA polymerase III–transcribed genes in budding yeast

Praveen Belagal[a], Christophe Normand[a], Ashutosh Shukla[b], Renjie Wang[a], Isabelle Léger-Silvestre[a], Christophe Dez[a], Purnima Bhargava[b,*], and Olivier Gadal[a,*]
[a]Laboratoire de Biologie Moléculaire Eucaryote, Centre de Biologie Intégrative, Université de Toulouse, CNRS, UPS, 31000 Toulouse, France; [b]Centre for Cellular and Molecular Biology, Council of Scientific and Industrial Research, Hyderabad 500007, India

ABSTRACT **The association of RNA polymerase III (Pol III)–transcribed genes with nucleoli seems to be an evolutionarily conserved property of the spatial organization of eukaryotic genomes. However, recent studies of global chromosome architecture in budding yeast have challenged this view. We used live-cell imaging to determine the intranuclear positions of 13 Pol III–transcribed genes. The frequency of association with nucleolus and nuclear periphery depends on linear genomic distance from the tethering elements—centromeres or telomeres. Releasing the hold of the tethering elements by inactivating centromere attachment to the spindle pole body or changing the position of ribosomal DNA arrays resulted in the association of Pol III–transcribed genes with nucleoli. Conversely, ectopic insertion of a Pol III–transcribed gene in the vicinity of a centromere prevented its association with nucleolus. Pol III–dependent transcription was independent of the intranuclear position of the gene, but the nucleolar recruitment of Pol III–transcribed genes required active transcription. We conclude that the association of Pol III–transcribed genes with the nucleolus, when permitted by global chromosome architecture, provides nucleolar and/or nuclear peripheral anchoring points contributing locally to intranuclear chromosome organization.**

Monitoring Editor
Karsten Weis
ETH Zurich

Received: Mar 4, 2016
Revised: Aug 10, 2016
Accepted: Aug 18, 2016

INTRODUCTION

Eukaryotic chromatin is a complex three-dimensional (3D) entity. Its organization within the nucleus can influence genome stability and gene expression (Misteli, 2007). Global genome organization in budding yeast has been clearly determined. The nucleolus, which is organized into a crescent-shaped structure adjacent to the nuclear envelope (NE), contains almost exclusively the genes encoding ribosomal DNA (rDNA) from the right arm of chromosome XII (Yang *et al.*, 1989; Léger-Silvestre *et al.*, 1999). In cycling cells, diametrically opposite the nucleolus, the kinetochore complex at the centromeres (CENs) is tethered to the spindle pole body (SPB) via microtubules throughout the cell cycle (Yang *et al.*, 1989; Bystricky *et al.*, 2005; Duan *et al.*, 2010; Zimmer and Fabre, 2011). Telomeres (TELs) are localized in clusters at the nuclear envelope (Klein *et al.*, 1992; Gotta *et al.*, 1996), such that the chromosome arms extend from the CEN toward the nucleolus and the nuclear periphery. Therefore, in cycling cells, chromosomes adopt a Rabl-like conformation (Jin *et al.*, 2000). Computational models based on small numbers of biophysical constraints and reproducing most of these features have recently been developed (Tjong *et al.*, 2012; Wong *et al.*, 2012; Gursoy *et al.*, 2014; Gong *et al.*, 2015). By studying budding yeast chromosome XII by live-cell imaging, we confirmed that the nuclear positions of loci were globally well predicted by such models (Albert *et al.*, 2013). Models introducing constraints due to nuclear biochemical activity have been reported to provide a better fit to experimental contact frequency maps (Gehlen *et al.*, 2012; Tokuda *et al.*, 2012). Recent imaging studies in different physiological conditions affecting the yeast transcriptome revealed a global shift of many positions on chromosome II to the periphery of the nucleus (Dultz *et al.*, 2016). This peripheral recruitment of

This article was published online ahead of print in MBoC in Press (http://www.molbiolcell.org/cgi/doi/10.1091/mbc.E16-03-0145) on August 24, 2016.

*Address correspondence to: Purnima Bhargava (purnima@ccmb.res.in), Olivier Gadal (gadal@biotoul.fr).

Abbreviations used: FROS, fluorescent repressor-operator system; MNase, micrococcal nuclease; PolI, RNA polymerase I; PolIII, RNA polymerase III; tDNA, tRNA-coding gene.

chromosome arms is consistent with the presence of transcription-dependent anchoring points along the length of the chromosome (Tjong *et al.*, 2012). However, the tethering sites organizing chromosomes locally remain largely unidentified (Dultz *et al.*, 2016).

Each of the three nuclear RNA polymerases transcribes a specific subset of genes. RNA polymerase (Pol) II transcribes all protein-coding genes and many noncoding (nc) RNA genes. Pol I synthesizes only one type of RNA—the precursor of large rRNAs. Pol III specializes in the synthesis of a few hundred ncRNAs, mostly involved in translation: the 5S rRNA, tRNAs, and abundant small ncRNAs. There is a well-documented correlation between the frequent association of a gene with a nuclear substructure and its transcriptional activity (Takizawa *et al.*, 2008). Pol I transcription is the model system for this preferential localization of genes. Indeed, assembly of the nucleolus, the largest nuclear body, is initiated by rDNA transcription by Pol I (Trumtel *et al.*, 2000; Misteli, 2001; Hernandez-Verdun *et al.*, 2002). Previous studies suggested that nucleolar association of Pol III-transcribed genes has been conserved during evolution. Nucleolus-associated domains in metazoan genomes are significantly enriched in tRNA genes (tDNAs; Nemeth *et al.*, 2010). In budding yeast, tDNAs scattered over the various chromosomes appear to be colocalized in a cluster close to or within the nucleolus on fluorescence in situ hybridization (FISH) microscopy (Thompson *et al.*, 2003; Haeusler and Engelke, 2004). Recent studies of budding yeast also reported transcription-dependent recruitment of a tDNA to the nuclear pore complex (NPC) during mitosis (Chen and Gartenberg, 2014). Pol III–transcribed genes may behave as local tethering sites for the organization of chromosome arms.

In this study, we investigated the intranuclear position of individual Pol III–transcribed genes in three dimensions. We measured distances from genes of interest to both nuclear and nucleolar centers (Berger *et al.*, 2008). FISH studies previously demonstrated a concentration of tRNA gene families (*Leu(CAA)*; *Lys(CUU)*, *Gly(GCC)*, *Gln(UUG)*, and *Glu(UUC)*) in or near the nucleolus (Thompson *et al.*, 2003). We used fluorescent operator-repressor system (FROS) insertion to label individual Pol III–transcribed genes and determine their position within the nucleus in vivo (Berger *et al.*, 2008). We found that some, but not all, Pol III–transcribed genes were frequently associated with the periphery of the nucleolus and/or away from the nuclear center. Proximity to the centromere or telomere prevented nucleolar recruitment, suggesting a hierarchical organization of locus positions. Centromere proximity constrained loci to be at the nuclear periphery close to SPB. Telomere proximity precluded central localization in the nucleus, resulting in loci close to SPB for short-arm chromosomes or away from SPB for long-arm chromosomes (Therizols *et al.*, 2010). Centromere inactivation or the insertion of a centromere at an ectopic site at some distance from a tDNA resulted in the nucleolar association of the Pol III—transcribed gene; peripheral position was kept, but shifted away from SPB toward the nucleolus. The nucleolar association of tDNA was alleviated by nutrient starvation, which inhibits Pol III transcription, However, Pol III transcription was not limited to nucleolus-associated genes. We evaluated the contribution of the gene itself to the intranuclear positioning of its host locus and showed that Pol III–transcribed genes controlled the local organization of the chromosome arms via nucleolar and/or nuclear envelope tethering.

RESULTS

Identification of Pol III–transcribed genes generating unique, detectable transcripts

Pol III–transcribed genes can be classified into three groups, types I–III, on the basis of their internal promoter organization (Figure 1A). Most tRNAs are encoded by large multigene families scattered throughout the yeast genome, with a mean of four genes encoding the same tRNA and up to 16 genes for *Gly(GCC)*. Even within multigene families, the isogenes encoding different tRNAs display very high levels of sequence identity, making it difficult to design gene-specific probes for estimating the abundance of a specific transcript. Furthermore, within a set of tRNA genes encoding the same anticodon, individual copies are not equivalent, and the deletion of individual genes may affect yeast fitness to very different extents (Bloom-Ackermann *et al.*, 2014). We performed a comprehensive survey to identify base-pair polymorphisms in tRNA sequences in each of the 20 families. In total, 69 tRNA species are produced from the 273 tDNAs of the yeast nuclear genome (Figure 1B, circles). We identified 33 unique tRNA species (circles labeled with 1 in Figure 1B) produced from single genes. Six of these 33 unique tDNAs bore unique anticodons. However, if a unique anticodon-encoding gene is lost, other tRNAs can decode the codon through wobble base pairing; as a result, only four of these six genes were considered essential (Bloom-Ackermann *et al.*, 2014).

We mapped 13 representative loci from the 278 different Pol III–transcribed genes in yeast by in vivo microscopy (gene names in blue in Figure 1B). We previously determined the intranuclear positions of 5 of these loci on chromosome XII: *SNR6*, the 5S gene in rDNA, and three tDNAs (*tP(UGG)L*, *tA(UGC)L*, and *tL(UAA)L*; Albert *et al.*, 2013). We explored the positions of Pol III–transcribed genes further by labeling *SCR1* (the gene encoding the RNA component of the signal recognition particle [SRP]) and seven other tDNAs: three of the four essential tDNAs (*TRT2*, *SUP61*, and *TRR4*) and *tG(CCC)*, represented by only two tDNAs—*SUF3* and *SUF5*—which display low but significant levels of sequence polymorphism (see later discussion). We also labeled *SUP4*, the deletion of which causes a strong growth defect, despite its membership in the large *tY(GUA)* family, which contains eight isoforms (Bloom-Ackermann *et al.*, 2014). The *SUP53* tDNA, for which expression can be assessed indirectly from the suppressor activity of a nonsense mutation (unpublished data), was also included in our study.

Intranuclear position of Pol III–transcribed genes

We determined the positions of individual Pol III–transcribed genes in the nuclear space in vivo by FROS labeling (TetO/TetR–green fluorescent protein [GFP]). The linear position of each gene on the chromosomes is shown in Figures 2A and 3A. We previously showed that, for Pol III–transcribed genes, a single nucleosome dynamics upstream for *SNR6* and downstream for tDNAs controlled differences in transcription (Arimbasseri and Bhargava, 2008; Mahapatra *et al.*, 2011; Kumar and Bhargava, 2013). The positions of FROS insertions close (from 60 to 800 base pairs) to genes of interest were therefore selected with care to ensure that the FROS insertion point affected neither adjacent nucleosome occupancy nor RNA Pol III recruitment. Pol III occupancy in the vicinity of tDNAs was assessed by chromatin immunoprecipitation (ChIP) and quantitative PCR (qPCR). Nucleosome position was determined by mononucleosome MNase protection assays, followed by qPCR. Pol III occupancy and nucleosome positioning were similar in the untagged and tagged cells (Supplemental Figure S1).

Gene position was determined by the NucLoc method (Berger *et al.*, 2008; Therizols *et al.*, 2010). Images were acquired from living, exponentially growing cells in culture by the confocal fluorescence imaging of large numbers of nuclei (>1000). Images were analyzed with dedicated software (see *Materials and Methods*). Briefly, for each cell with a spherical nucleus (including the G1, S, and early G2/M phases), nuclear and nucleolar volumes were determined on the basis

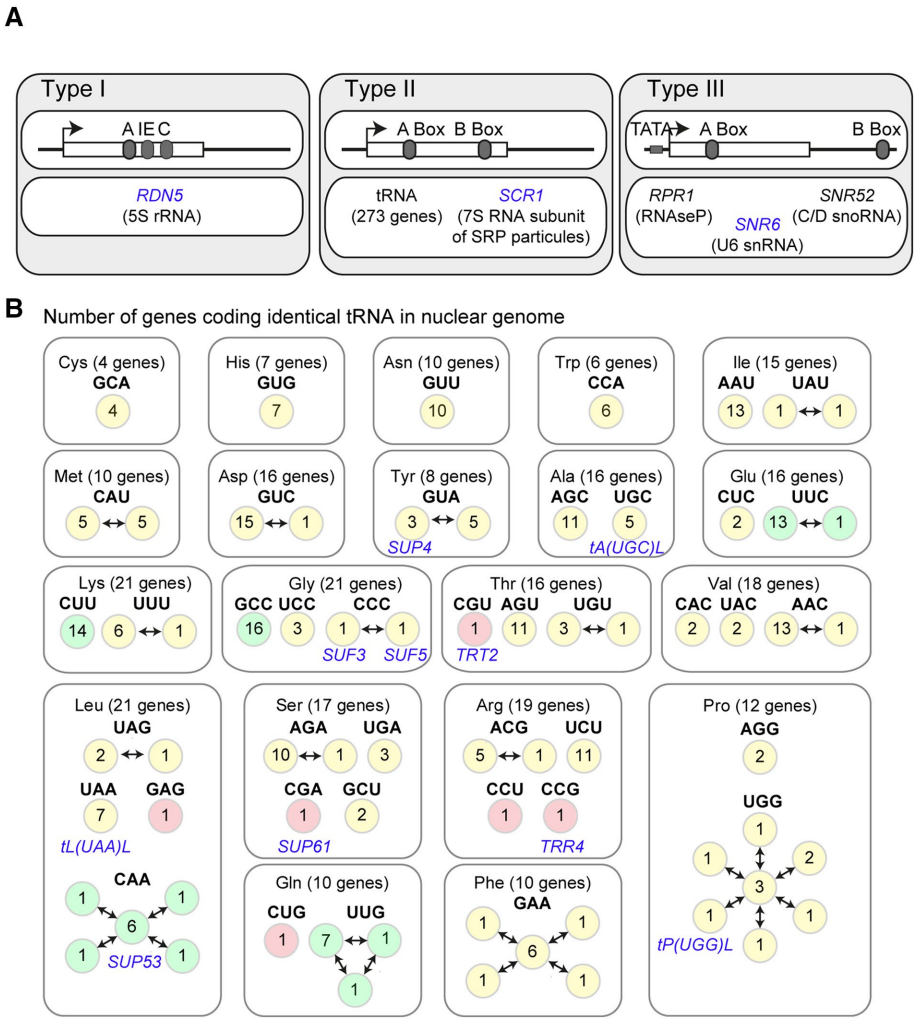

FIGURE 1: Schematic representation of Pol III–transcribed genes. (A) Pol III–transcribed genes can be classified on the basis of internal promoter organization into types I–III. Positions of boxes A, IE, B, and C (gray oval) relative to the transcription start site (arrow) and the transcribed region (rectangle). (B) It is challenging to find individual tRNA genes (tDNAs) to label from which a unique gene product can be unambiguously identified. The 273 tDNAs generate 69 different tRNAs (circles) in budding yeast. Each family, defined on the basis of the amino acid targeted (rectangles) and the anticodon (bold), contains 1–16 genes (colored circles and numbers of identical genes). Double arrows link tRNAs within a family responsible for decoding the same anticodon but with different sequences. Unique genes for the decoding of a specific anticodon are shown in red and those with a known nucleolar distribution (Thompson *et al.*, 2003) in green. The FROS used for labeling was inserted near the genes highlighted in blue.

of the fluorescent Nup49-GFP (nuclear pore complex) and Nop1-mCherry (nucleolar protein) signals, respectively. Locus position was determined relative to two references: the 3D positions of the centers of the nucleus and the nucleolus. Nucleus geometry was explored by measuring the angle (α) between the locus–nuclear center axis and the nuclear center–nucleolar center axis. By construction, nucleolar center is at $\alpha = 180°$. SPB is peripheral and opposed to the nucleolus ($\alpha \approx 0$). Peripheral location of a locus away from SPB will result in a larger α (~45–180°). The distance between the locus and the nuclear center was used, together with α, to generate a color-coded statistical map of locus positions in which the percentage indicated within a contour represents the probability of finding the locus within that contour. On these maps, the average nuclear circumference is depicted as a yellow circle, and the median nucleolus (including 50% of all nucleoli) is displayed as a red isocontour (see Figures 2B and 3B).

The previously characterized intranuclear positions of the 5S rDNA and *SNR6* gene loci (Albert *et al.*, 2013) are shown in Figure 2B. As expected, 5S rDNA, which is interspersed with RNA polymerase I–transcribed rRNA gene repeats (35S rDNA) in the budding yeast genome, was restricted to the nucleolus (Figure 2B; Berger *et al.*, 2008; Albert *et al.*, 2013). The *SNR6* locus, which is located 86 kb away from the rDNA, toward the centromere on the right arm of chromosome XII, appeared to be mostly localized at the nucleolar periphery. We also determined the intranuclear positions of two tDNA loci: *SUP53* and *SUP4*. A transcriptionally active *SUP53* gene has been reported to be associated with the nucleolus (Thompson *et al.*, 2003). Using our FROS strain, we found that *SUP53*, which is located 23 kb from the centromere on the left arm of chromosome III, was excluded from nucleolar periphery, whereas *SUP4*, sited 107 kb from the centromere on the right arm of chromosome X, was detected in a large volume within the nuclear space, frequently interacting with the nucleolus (Figure 2B). Similarly, *SUF3* and *SUF5*, both located >250 kb from the centromere and telomere, were frequently found to be associated with the nucleolar periphery. We found that *SUF3* was also frequently located in the periphery of the nucleus. The 5S rRNA gene, *SUP4*, *SUP53*, *SUF3*, and *SUF5* all belong to multigene families in which functionally equivalent transcripts can be produced from multiple genes, and so it was not possible to determine the proportion of transcriptionally active genes among the loci localized.

We next localized three essential tDNAs (*TRT2*, *TRR4*, and *SUP61*) with unique anticodons as transcriptionally active Pol III loci. We also determined the position of *SCR1*, an essential non-tRNA Pol III transcript (Figure 3, A and B). The genomic positions of the loci are shown in Figure 3A, and localization maps are displayed in Figure 3B. *TRT2* is located close to the left telomere (47 kb) on chromosome XI and was found to have a perinuclear distribution reminiscent of subtelomeric sequences, rarely coming into contact with the nucleolus (Therizols *et al.*, 2010). The *TRR4* locus is located 350 kb from the rDNA and 261 kb from the right telomere, on the right arm of chromosome XII. *TRR4* nuclear position appears both at the nucleolar and nuclear periphery. *SCR1* is located on the right arm of chromosome V, 290 kb from CEN and 135 kb from the telomere. Like *SUF3* and *TRR4*, *SCR1* was preferentially associated with the nucleolus and nuclear periphery. *SUP61* is located 113 kb from the centromere and it appeared to be excluded from the nucleolar periphery, in close proximity to the nuclear envelope. Both *SUP4* and *SUP61* are located ~100 kb from centromere, but the maps of these genes were markedly different. *HMR*, a heterochromatin domain attached to the nuclear envelope, is located 66 kb from the *SUP61* locus.

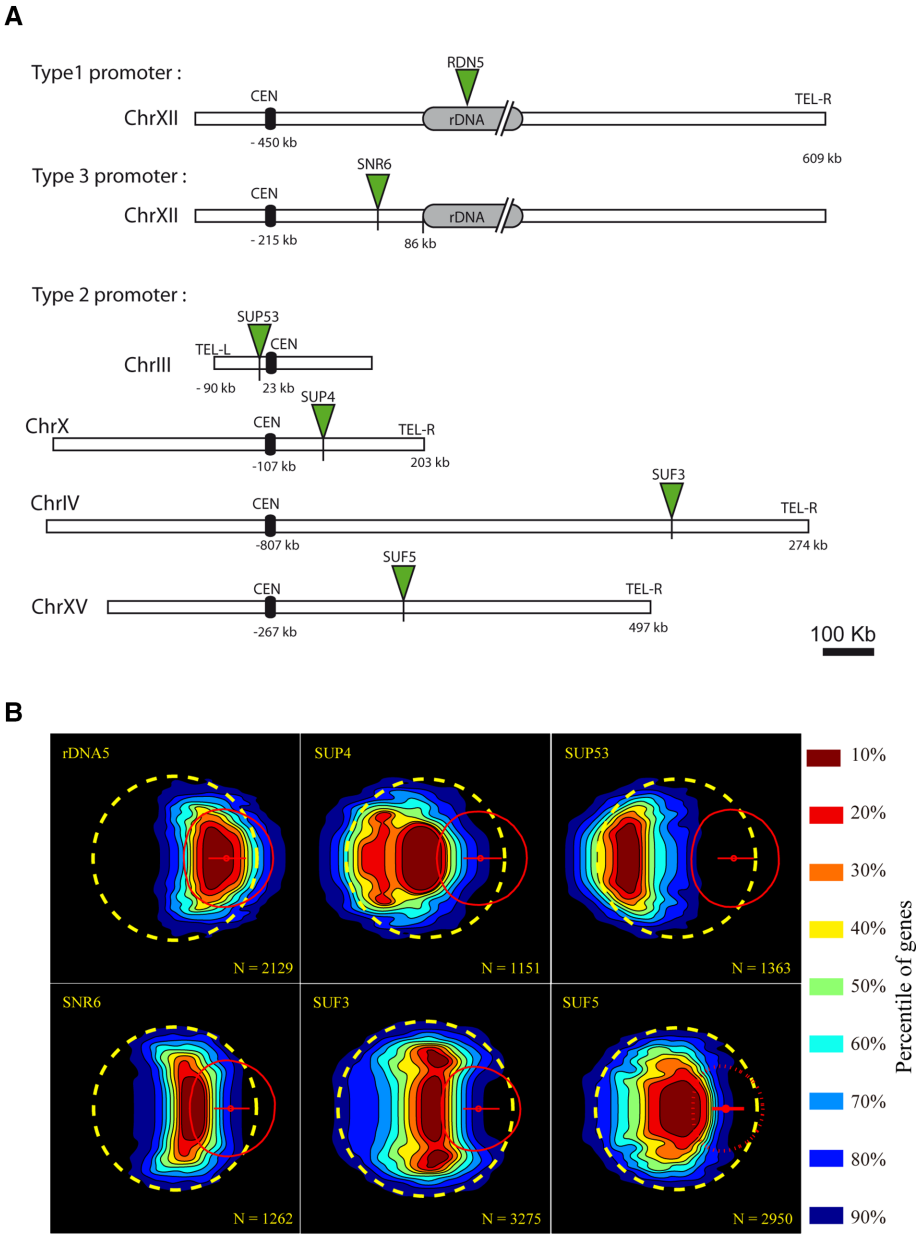

FIGURE 2: Positions of Pol III–transcribed genes on the chromosomes and in the intranuclear space. (A) FROS insertions near *RDN5, SNR6, SUP53, SUP4, SUF3*, and *SUF5* genes on the chromosome relative to CEN, rDNA, and left and right TELs. The distance of the FROS insertion (green triangle) relative to the two closest tethering elements (kilobases) is indicated. (B) Gene map of the FROS-labeled loci. Yellow circle and red ellipsoids correspond to nuclear envelope and nucleolus, respectively. *N*, number of nuclei used to generate the probability density map. The probability of finding the locus within the various regions of the nucleus is indicated by the percentage enclosed within the contour concerned.

SUP61, *tT(UGU)G1*, and *tT(AGU)C* were recently reported to be preferentially associated with the NPC during mitosis (Chen and Gartenberg, 2014). We explored the possible cell cycle–regulated positioning of another Pol III–transcribed gene, *SCR1*. In our aggregate population analysis, *SCR1* was preferentially found in two positions: nucleolus and nuclear periphery (Figure 3B). We manually sorted nuclei by cell shape to analyze G1 (unbudded), S (small buds), and G2/M (choosing large buds with round nuclei, excluding anaphase) phases. Perinucleolar recruitment was observed mostly in G1 (Figure 3C, left). Marked recruitment to the nuclear periphery was observed in S phase and conserved in G2/M (Figure 3C, middle and right).

A comparative analysis of all the intranuclear maps of Pol III–transcribed genes in this study (Table 1) showed that the close proximity of tethering elements (<100 kb from CEN, TEL, or HMR) prevented the association of Pol III–transcribed genes (*SUP53*, *TRT2*, and *SUP61*) with the nucleolus. Conversely, the close proximity of *SNR6* to rDNA on the right arm of chromosome XII was associated with an exclusively nucleolar location. For regions with no obvious constraints on their motion due to the Rabl-like chromosomal architecture, Pol III–transcribed genes displayed frequent, possibly cell cycle–regulated nucleolar interactions (*SUP4* and *SUF5*) or nucleolar/nuclear periphery interactions (*SRC1*, *TRR4*, and *SUF3*).

Proximity to centromeres prevents the association of Pol III–transcribed genes with nucleoli

Our mapping results suggest that the proximity of genes to tethering elements such as centromeres prevents them from associating with nucleoli. We investigated the interplay between Pol III–transcribed genes and centromeres, using a genetic system for the ectopic insertion of any gene at the *SUP53* locus, which is close (23 kb) to the centromere (Supplemental Figure S2). Because the SPB occupies a position diametrically opposite to that of the nucleolus, we hypothesized that proximity to the centromere would result in the locus being tethered away from the nucleolus. We changed the genomic locations of four Pol III–transcribed genes from the three Pol III classes: the 5S rRNA gene (type 1), one tDNA (*SUF3*), and two essential type III genes (*SNR6, SCR1*; Figure 4A). All were strongly associated with the nucleolus when in their wild-type genomic positions (Figure 4B, top). No growth defect was detected in any of the strains carrying an ectopic gene at the *SUP53* locus with deletion of the gene at its endogenous wild-type locus (unpublished data). We mapped each ectopic insertion and compared it to the wild-type position of the gene (Figure 4B, compare top to bottom). We observed no nucleolar recruitment for *SUF3*, *SNR6*, and *SCR1* inserted at the *SUP53* locus close to the centromere. In the budding yeast genome, the 5S rDNA is inserted between copies of the Pol I–transcribed rDNA repeat (35S rDNA). This organization is unusual, in that 5S rDNA arrays are clustered into arrays separately from the 35S rDNA in other organisms. In fission yeast, the insertion of a 35S rDNA sequence not including the 5S rDNA at the mating-type region induced relocalization of the gene from the SPB to the nucleolar periphery (Jakociunas *et al.*, 2013). The 5S rDNA (*RDN5*) gene is universally associated with nucleoli (Haeusler and Engelke, 2006). We therefore hypothesized that a single 5S rDNA at the *SUP53* locus would drive strong nucleolar association. However, the insertion of

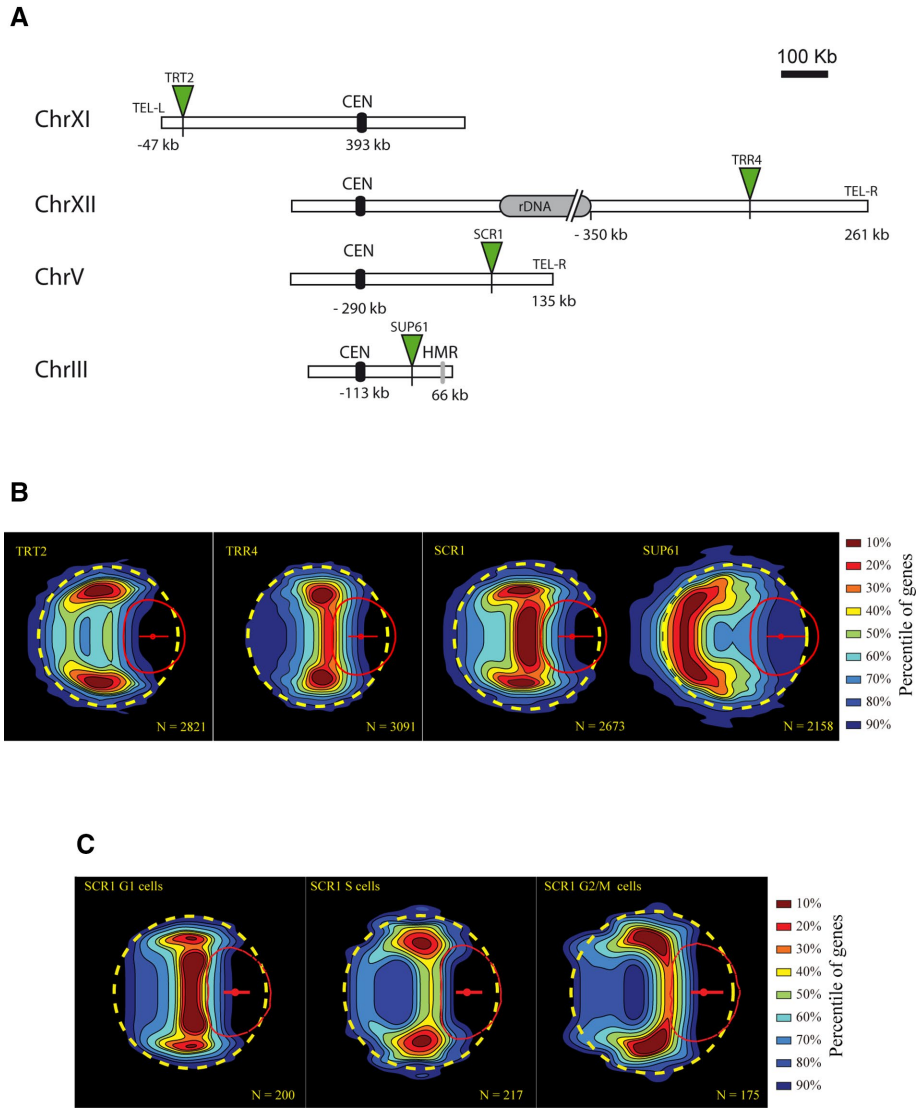

FIGURE 3: Positions of four essential Pol III–transcribed genes on chromosomes and in the intranuclear space. (A) FROS insertions near *TRT2, TRR4, SCR1*, and *SUP61* genes on the chromosome relative to *CEN*, rDNA, right and left TELs, and silent mating-type loci (*HMR*). The distance of the FROS insertion (green triangle) from the two closest tethering elements (kilobases) is indicated. (B) Gene map of the FROS-labeled loci. Yellow circle and red ellipsoids correspond to nuclear envelope and nucleolus, respectively. *N*, number of nuclei used to generate the probability density map. (C) Gene map of the FROS-labeled *SCR1* gene during the cell cycle.

RDN5 at *SUP53* was not sufficient to drag the locus to the nucleolus (Figure 4B, rightmost images). The identity of the Pol III–transcribed gene inserted in place of *SUP53* did not affect the intranuclear position of the locus (Figure 4C).

Our data suggest that the Pol III–transcribed genes tested could not direct the association of a centromere-proximal region to the nucleolar periphery or significantly modify gene position relative to that of the wild-type *SUP53* gene.

Pol III–transcribed SUP53 slides along the nuclear periphery toward the nucleolus when the chromosome III centromere is inactivated or displaced

The Pol III–transcribed, centromere-proximal *SUP53* locus is not found near the nucleolus in wild-type cells. We disrupted *CEN* function to determine whether CEN proximity (23 kb) prevented nucleolar association. We used a strong inducible promoter (*pGAL1-10*) to disengage the kinetochore from the centromere (Hill and Bloom, 1987; Reid *et al.*, 2008). On induction, GAL genes were recruited to the nuclear periphery, as previously reported (Casolari *et al.*, 2004). We inserted the *pGAL1-10* promoter at the chromosome III centromere (*CEN3*), close to *SUP53* (Figure 5A). Expression under *pGAL1-10* control caused a conditional knockdown of *CEN3* kinetochore attachment, strongly decreasing cell viability upon induction (Figure 5B), due to chromosome segregation defects resulting from kinetochore disassembly. As control, we checked that the wild-type *SUP53* locus position was unaffected by shifting the cells from repressed to induced conditions for up to 4 h (Figure 5C, left). We then induced *CEN3*–kinetochore dissociation using similar growth conditions and monitored locus positions (Figure 5C, middle). The location of *SUP53* was significantly affected by *CEN3*–kinetochore dissociation, with this locus predominantly occupying a peripheral position. The nucleolar recruitment of *SUP53* did not increase significantly even after 4 h of induction. *CEN3* kinetochore inactivation significantly modified the angle α between the locus–nuclear center axis and the central axis (Figure 5C, right). This angle was unaffected in wild-type (WT) cells incubated with galactose for 4 h (Figure 5D, left) but gradually increased after kinetochore disassembly (Figure 5D, right). *SUP53* thus remained at the nuclear periphery, appearing to deviate from the axis between the nuclear and nucleolar centers. No such effect was observed if a centromere other than *CEN3* was disrupted (*CEN9*; Supplemental Figure S3). It was not possible to explore longer periods of *CEN3* release due to cell morphology abnormalities. We overcame this problem by constructing a strain in which the endogenous *CEN3* was deleted and an ectopic centromere (*CEN6*) was inserted 14.2 kb from *TEL-R* and 212 kb from *SUP53* (Figure 5E, left). This strain displayed no growth defect (Supplemental Figure S3C). After permanent centromere release, *SUP53* gene was recruited to the nuclear and nucleolus periphery (Figure 5E, right). These results confirm that proximity to the centromere constrains the location of *SUP53*.

An ectopic location of rDNA alters the nucleolar association of Pol III–transcribed genes

SNR6 had a strictly perinucleolar location (Figure 2B). We suggest that this is largely due to the proximity of rDNA and *SNR6* (only 86 kb apart), anchoring the locus to the nucleolus. We tested this hypothesis by modifying a strain constructed by M. Nomura's laboratory, rDNA-CEN5, for gene position analysis. In this strain, all of the rDNA repeats of chromosome XII have been deleted

Reference	Gene name	Common name	Genomic location: +rDNA = 1–2 Mb of rDNA array				Nuclear location
			Chromosome number	Distance			
				CEN	rDNA	Other	
Albert *et al*. (2013)	*RDN5*	5S rRNA gene	XII	309 kb right	Inside	588 kb + rDNA from right telomere	Away from SPB; inside nucleolus
Albert *et al*. (2013)	*SNR6*	U6 snRNA gene	XII	216 kb right	86 kb left	674 kb + rDNA from right telomere	Away from SPB; nucleolar periphery
Albert *et al*. (2013)	*tP(UGG)L*	None	XII	58 kb left	359 kb left	93 kb from left telomere	Nucleoplasm
Albert *et al*. (2013)	*tA(UGC)L*	None	XII	64 kb right	237 kb left	261 kb from right telomere	Away from SPB; nucleoplasm/ nucleolar periphery
Albert *et al*. (2013)	*tL(UAA)L*	None	XII	812 kb + rDNA left	473 kb right	115 kb from right telomere	Away from SPB; nucleolar and nuclear periphery
This study	*tR(CCG)L*	*TRR4*	XII	668 kb + rDNA left	350 kb right	261 kb from right telomere	Away from SPB; nucleolar and nuclear periphery
This study	*SCR1*	7SL RNA gene	V	290 kb right	Not linked	135 kb from right telomere	Away from SPB; nucleolar and nuclear periphery
This study	*tL(CAA)C*	*SUP53*	III	23 kb	Not linked	90 kb from left telomere	Close to SPB, nuclear periphery; away from nucleolus
This study	*tS(CGA)C*	*SUP61*	III	113 kb right	Not linked	66 kb left of HMR locus	Close to SPB, nuclear periphery; away from nucleolus
This study	*tY(GUA)J2*	*SUP4*	X	107 kb	Not linked	203 kb from right telomere	Away from SPB; nucleoplasm/ nucleolar periphery
This study	*tG(CCC)D*	*SUF3*	IV	807 kb right	Not linked	274 kb from right telomere	Away from SPB; nucleolar and nuclear periphery
This study	*tT(CGU)K*	*TRT2*	XI	393 kb	Not linked	47 kb from left telomere	Nuclear periphery
This study	*tG(CCC)O*	*SUF5*	XV	267 kb	Not linked	765 kb from right telomere	Nucleolar periphery

TABLE 1: Gene-mapping results for Pol III–transcribed genes in the budding yeast nucleus.

and reinserted in the vicinity of the centromere on chromosome V (see *Materials and Methods* and Figure 6A; Oakes *et al*., 2006). As previously observed, the nucleolus was located diametrically opposite the SPB in the WT strain (Figure 6B; bottom). After ectopic rDNA insertion, the SPB was close to the nucleolus (Figure 6B, top; Oakes *et al*., 2006). The rDNA-CEN5 strain had impaired growth, and the nuclear radius was increased, making distance variation difficult to interpret. We explored the changes in nucleus geometry using the gene map and the α angle variation, which remains informative even if nucleus size is modified. In the rDNA-CEN5 strain, *SUP53* was confined to the nucleolar periphery (Figure 6C, left). In the rDNA-CEN5 strain, *SNR6* was not linked to rDNA and was located 215 kb from the centromere and 648 kb from the right telomere (Figure 6A). *SNR6* was more widely dispersed in the nucleus in the mutant rDNA-CEN5 strain than in the WT strain (Figure 6C, right). Its geometric position in these two strains could be described by the α angle distribution. In the WT strain, the distribution of α angles was centered on 105°, reflecting a perinucleolar location (Figure 6D). The distribution of α angles was broader and centered on 75° in the rDNA-CEN5 strain, reflecting a displacement of the locus away from the nucleolus. Therefore, in the rDNA-CEN5 strain, *SNR6* was not strictly perinucleolar but nevertheless remained frequently associated with the nucleolus, confirming that Pol III–transcribed genes located away from anchoring elements often interact with the nucleolar periphery.

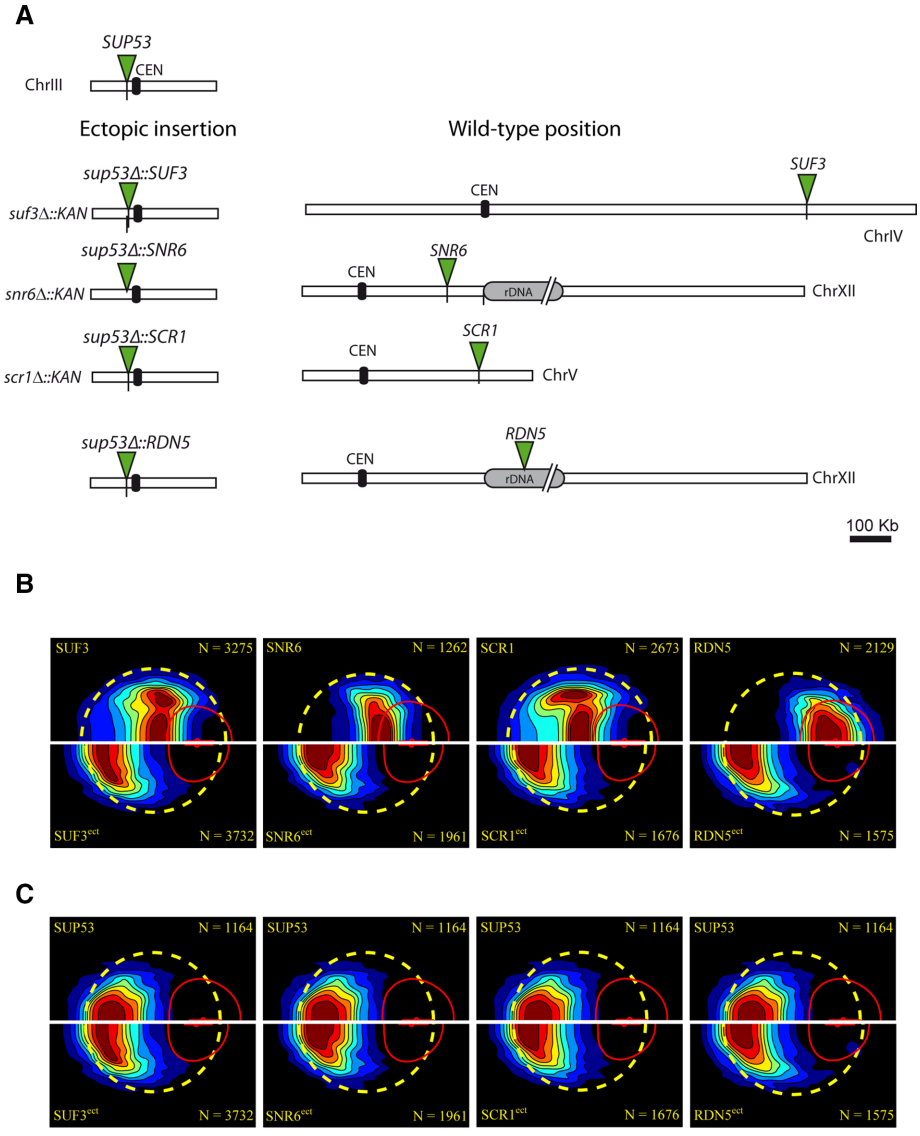

FIGURE 4: Positions of ectopically inserted genes. (A) Description of ectopic strains. *SNR6*, *SCR1*, *SUF3*, and a copy of *RDN5* were inserted separately at the *SUP53* locus. Except for *RDN5*, for which there are ~200 copies, the original copy of the inserted gene was deleted. (B) Gene maps for the original locus and the ectopic *SUP53* location for the *SNR6*, *SCR1*, *SUF3*, and *RDN5* genes. (C) Gene maps for *SUP53* at its native position and for ectopic insertions of *SNR6*, *SCR1*, *SUF3*, and *RDN5* at the *SUP53* locus (top and bottom, respectively).

Nucleolar association is not essential for the expression of Pol III–transcribed genes

We investigated the link between expression and the location of Pol III–transcribed genes in the nuclear space by comparing expression levels for *SNR6*, *SCR1*, and a tDNA, *SUF3*, in their wild-type (nucleolus-associated) and ectopic (close to the centromere, excluded from the nucleolar periphery) positions (Figure 7).

SNR6 and *SCR1* are single-copy genes. We used Northern blotting to determine the levels of their transcripts relative to those of an abundant Pol II transcript (snR46). *SNR6* and *SCR1* transcript levels were not affected by a change in the position of the locus within the genome (compare WT and ectopic, Figure 7, A and B). For *SCR1*, as a control, we evaluated transcript levels before and after FROS insertion. No change in transcript level was detected (Figure 7B, lane 2 vs. lane 3). Finally, we assessed the dependence of *SUF3* tDNA expression level on nucleolar association by primer extension (Figure 7C). As loading control, we designed a probe (o-Gly) for assessing overall RNA levels for 18 of the 21 tDNAs of the glycine family. We tried to generate a probe targeting either the *SUF3* or *SUF5* tRNA based on two polymorphisms found in *SUF3* and *SUF5* (Figure 7C, top). Gene-specific transcript levels were determined with total RNA from the WT, *suf3Δ*, and *suf5Δ* strains. The *SUF5* probe did not appear to be specific, whereas the *SUF3* signal was ~70% lower in the *suf3* deletion mutant than in wild type (no decrease in the *suf5* deletion mutant) and was therefore considered to display good specificity (Figure 7C, left). The ectopic insertion of *SUF3* away from the nucleolus had no major effect on transcript levels (Figure 7C, right). Thus Pol III–transcribed gene expression levels are not strictly dependent on nucleolar association.

Nontethered Pol III–transcribed genes drive association with the nucleolar periphery

Our results confirm that a Rabl-like chromosomal architecture constrains the spatial position of genes located close to centromeres and rDNA-anchoring elements. Furthermore, when not tethered by nearby structural elements, individual Pol III–transcribed genes are frequently associated with the nucleolar periphery.

We then investigated whether the association of the Pol III–transcribed locus *SUP4* with the nucleolus was directly dependent on Pol III activity. To distinguish between passive recruitment to the nucleolus and transcription-based recruitment, we cultured FROS-labeled cells for 2 h in dilute rich medium with no carbon source. This treatment efficiently shuts off Pol III transcription in vivo (Roberts *et al.*, 2003), as demonstrated by the release of Pol III from genes (Figure 8A; Kumar and Bhargava, 2013). This starvation treatment halved the ratio of nucleolar-to-nuclear volumes in strains carrying labeled *SNR6*, *SUP4*, and *SUP53* loci (Figure 8B), reflecting a decrease in nucleolar volume in the absence of a change in nuclear volume. A decrease in nucleolar size is also observed when the global reprogramming of transcription is induced by rapamycin treatment, with only a minor effect on overall chromosome architecture (Albert *et al.*, 2013).

We compared locations of the *SUP4* gene in expressed and nonexpressed conditions and of loci tethered by a centromere (SUP53) or close to rDNA (SNR6) as controls. The distance of the *SUP4* locus from the nucleolar center was modified in starved cells (Figure 8C). We quantified the observed effect by plotting the cumulative frequency distribution of distances between the loci and the center of the nucleolus and comparing normal and starvation conditions (Figure 8D, solid and dashed lines, respectively). No significant difference was detected for the centromere-associated locus *SUP53* (two-sample Kolmogorov–Smirnov test [ks-test2],

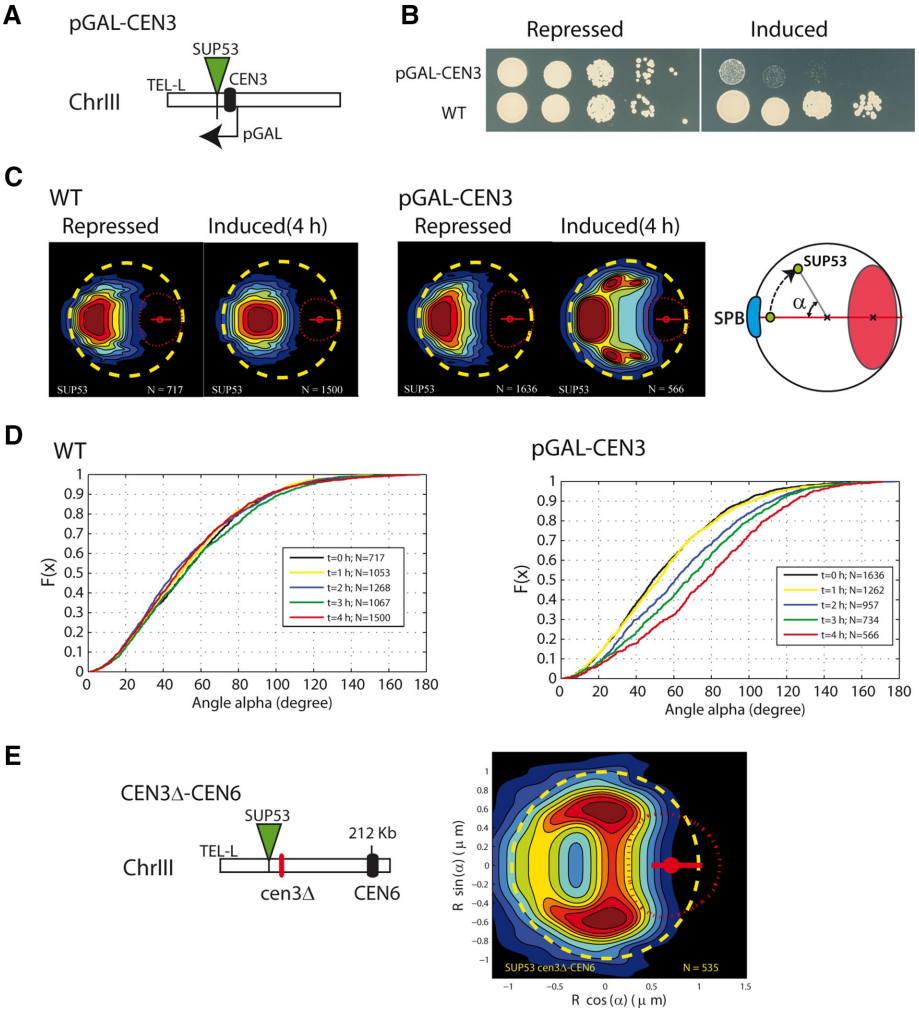

FIGURE 5: Releasing *CEN3* from the SPB results in *SUP53* relocalization. (A) Important features of chromosome III in pGAL-CEN3. (B) Evaluation of the growth of serial dilutions of WT and pGAL-CEN3 strains on media supplemented with glucose (repressed) or galactose (induced). (C) Gene map of the FROS-labeled *SUP53* locus in the WT (left) or pGAL-CEN3 (middle) in medium supplemented with glucose (repressed) and after 4 h of culture in medium supplemented with galactose (induced). Right, *SUP53* locus movement in galactose: the locus (green dot) deviates from the nuclear–nucleolar center axis (red line), resulting in an increase of α angle values. Red, nucleolus. Blue, positions occupied by the SPB. (D) Cumulative distribution function of the gene–nuclear center axis and the nuclear–nucleolar center axis angle α in WT (left) and pGAL-CEN3 (right) strains during the time-course experiment in galactose-supplemented medium. (E) Left, important features of chromosome III in the cen3Δ-CEN6 strain. Right, gene map of the FROS-labeled *SUP53* locus in the cen3Δ-CEN6 strain.

$p = 0.05$), consistent with CEN attachment to SPB, which is known to be independent of transcriptional inhibition (Albert *et al.*, 2013; Verdaasdonk *et al.*, 2013). The *SNR6* locus, located close to rDNA, appeared to be significantly (ks-test2, $p = 6 \times 10^{-13}$) closer to the center of the nucleolus (Figure 8D) after the change in nucleolar radius during starvation: mean nucleolar radius in the labeled strain was decreased from 0.7 to 0.5 μm by starvation (Figure 8D, light to dark gray). It has been shown that the decrease in nucleolar volume induced by rapamycin treatment results in a small but significant shift of locus positions toward the center of the nucleolus (Therizols *et al.*, 2010). However, *SUP4* did not follow this pattern, as it was located predominantly at the nucleolar periphery in glucose-containing medium and displayed a significant shift away from the nucleolar region upon nutrient stress (ks-test2; $p = 1 \times 10^{-6}$). This indicates that the association of *SUP4* with the nucleolus is driven by its transcription. Indeed, tRNA genes have been shown to dissociate from the nucleolus when transcription is abolished by promoter mutation (Thompson *et al.*, 2003).

For confirmation that the lower frequency of *SUP4* nucleolar association resulted directly from inhibition of the Pol III–mediated transcription of this gene rather than global reorganization due to glucose starvation, we deleted *SUP4* and monitored the position of the *sup4Δ* locus in glucose-rich medium. *SUP4* deletion resulted in a strong growth defect (unpublished data; Bloom-Ackermann *et al.*, 2014). Normal growth was restored by inserting an ectopic copy of the gene at *SUP53* locus (Figure 8E). *SUP4* gene deletion resulted in a greater distance between the deleted *SUP4* locus and the nucleolar center (Figure 8F; ks-test2; $p = 1.4 \times 10^{-12}$). Thus, in the cell population, the frequency of *SUP4* tDNA locus association with the nucleolar periphery depends on the presence of the gene. We then investigated the effects of deleting *SUF3*, *SUF5*, *SCR1*, *TRR4*, and *TRT2*, all located away from the tethering elements studied earlier (Supplemental Figure S4). All the deletions tested, except *SUF3*, induced a small but significant (ks-test2; $p = 10^{-3} - 10^{-9}$) shift of the locus away from the nucleolus. For *SUF3* tDNA, the perinuclear anchoring upon deletion of the tRNA gene was weakened.

In conclusion, our localization study confirmed that Pol III–transcribed genes located away from tethering elements were recruited to the nucleolus or its periphery. The association of the tDNA *SUP4* locus with the nucleolar periphery was specifically reduced by the inhibition of Pol III transcription or deletion of the gene. Nucleolar recruitment was observed for most of the genes tested. We also observed perinuclear anchoring of Pol III–transcribed genes away from tethering elements (i.e., *SUF3*). With the spectrum of genes studied here, we showed that Pol III–transcribed genes were able to tether the chromosome arm locally to either nuclear or nucleolar periphery.

DISCUSSION

The major finding of this study is that hierarchical constraints in chromosome organization control the position of Pol III–transcribed genes in the nucleus. The Rabl-like conformation of yeast chromosomes imposes a rigid scaffold that strongly modulates the frequency of associations between Pol III–transcribed genes and the nuclear and/or nucleolar periphery. Pol III–transcribed genes close to tethering elements, such as centromeres, HMR, or telomeres, interact with the nucleolus at very low frequency in cell populations. Here we confirmed that a locus near CEN is close to the NE and constrained by SPB, and a locus near TEL is at the NE. We showed that Pol III–transcribed genes located >100 kb from these

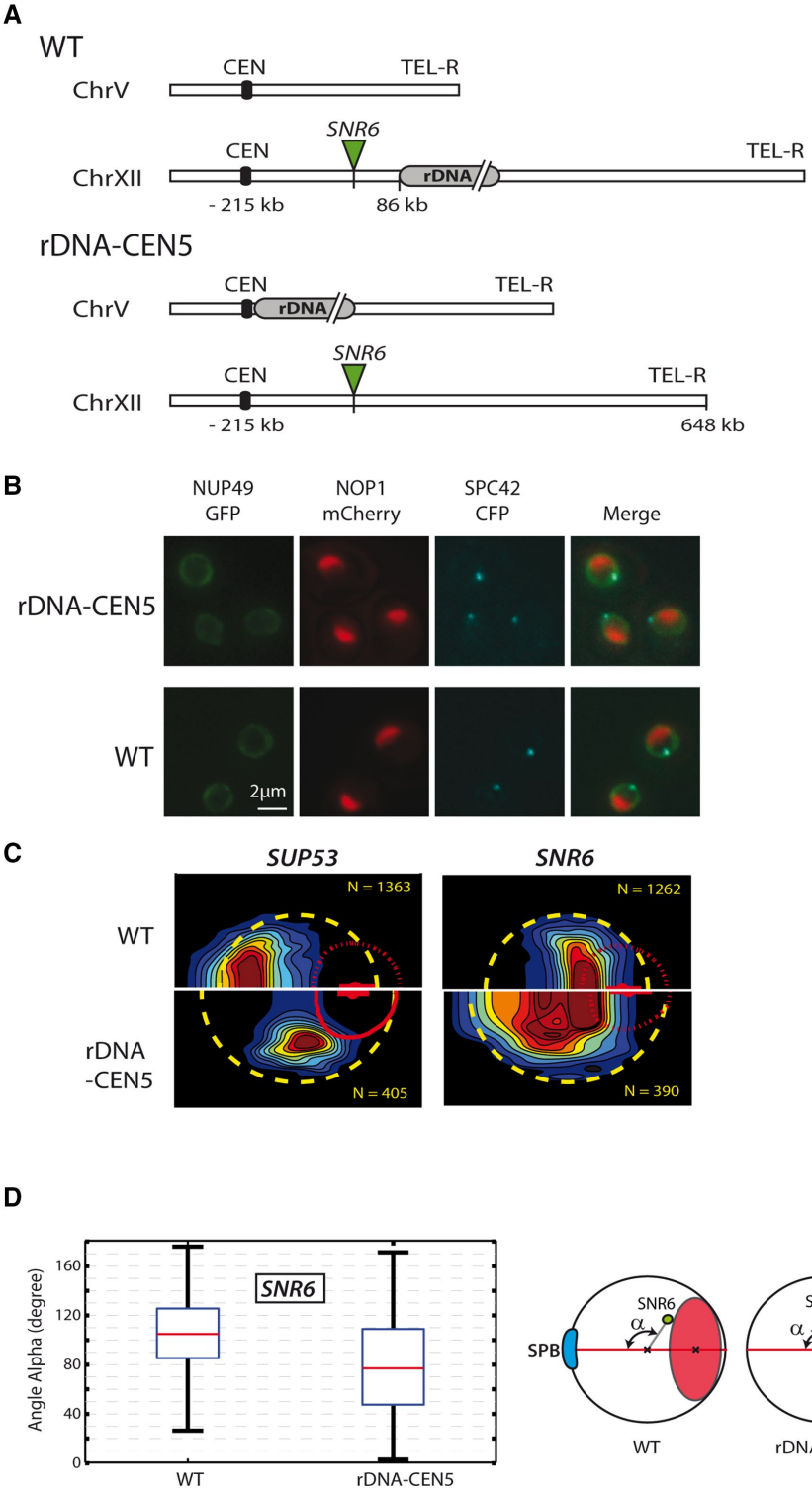

FIGURE 6: Ectopic insertion of rDNA modifies nucleolar associations. (A) Important chromosomal features in the WT and rDNA-CEN5 strains. (B) In vivo labeling of the SPB (SPC42-CFP, blue signal) and nucleolus (NOP1-mCherry) in the nucleus of the WT (left) and rDNA-CEN5 strains. (C) Gene map of the *SUP53* (left) and *SNR6* (right) loci in WT (top) and rDNA-CEN5 (bottom) strains. (D) Box plot of α angle distribution for *SNR6* locus in WT and rDNA-CEN5 strains. Median angle (for 20 individual nuclei) values. Red line, median α value. Edges of the box are 25th and 75th percentiles. Whiskers extend to 10th and 90th percentiles. Right, angle between *SNR6* locus (green dot) and nuclear–nucleolar center axis (red line). The region occupied by the SPB (blue) is close to the nucleolus in the rDNA-CEN5 strain.

tethering elements were frequently found close to the nucleolus and/or NE. Changing the position of genes relative to tethering elements (CEN and rDNA) allowed us to monitor the position of Pol III–transcribed genes free from constrains imposed by the Rabl-like configuration. Our results demonstrated that recruitment of a tDNA locus at the nucleolar periphery is driven by the Pol III–transcribed gene itself. Finally, for a subset of genes, we were also able to show that nucleolar association of the host locus depended on the presence of the Pol III–transcribed gene and was driven by its transcriptional status. For one case (*SUF3*), nucleolar association was not affected upon Pol III–transcribed gene deletion, but peripheral location was weakened.

Hierarchy of constraints driving chromosome organization in vivo

tRNA gene clustering at the nucleolus is believed to affect global chromosome folding in vivo, potentially competing with centromeric recruitment to the SPB (Haeusler and Engelke, 2006). We showed here, using ectopic insertions of essential Pol III–transcribed genes close to centromeres, that centromeric proximity prevented nucleolar recruitment of Pol III–transcribed genes. The genes studied included *SCR1* and *SNR6* genes, which can drive nucleolar recruitment. Permanent centromere release, manipulating *CEN3* location within the chromosome, was sufficient for the nucleolar recruitment of Pol III–transcribed genes. We conclude that the recruitment of Pol III–transcribed genes to the nucleolus or nuclear periphery contributes to higher-order chromosome organization in vivo when permitted by the strongest constraints imposed by the Rabl-like conformation.

Pol III–transcribed genes preferentially localize at the nuclear and nucleolar periphery

tRNA-encoding genes are recruited to the nuclear periphery in G2/M (Chen and Gartenberg, 2014), consistent with changes in the location of Pol III–transcribed genes during the cell cycle. We used yeast strains and automated data analysis methods developed primarily for the mapping, with high accuracy, of gene positions relative to the nucleolus. However, we were also able to demonstrate the frequent localization of *tL(UAA)L* (Albert *et al.*, 2013), *SUF3*, *TRR4*, and *SCR1* at the nuclear periphery. We found that *SCR1* was recruited to the nucleolar periphery mostly in G1. In the

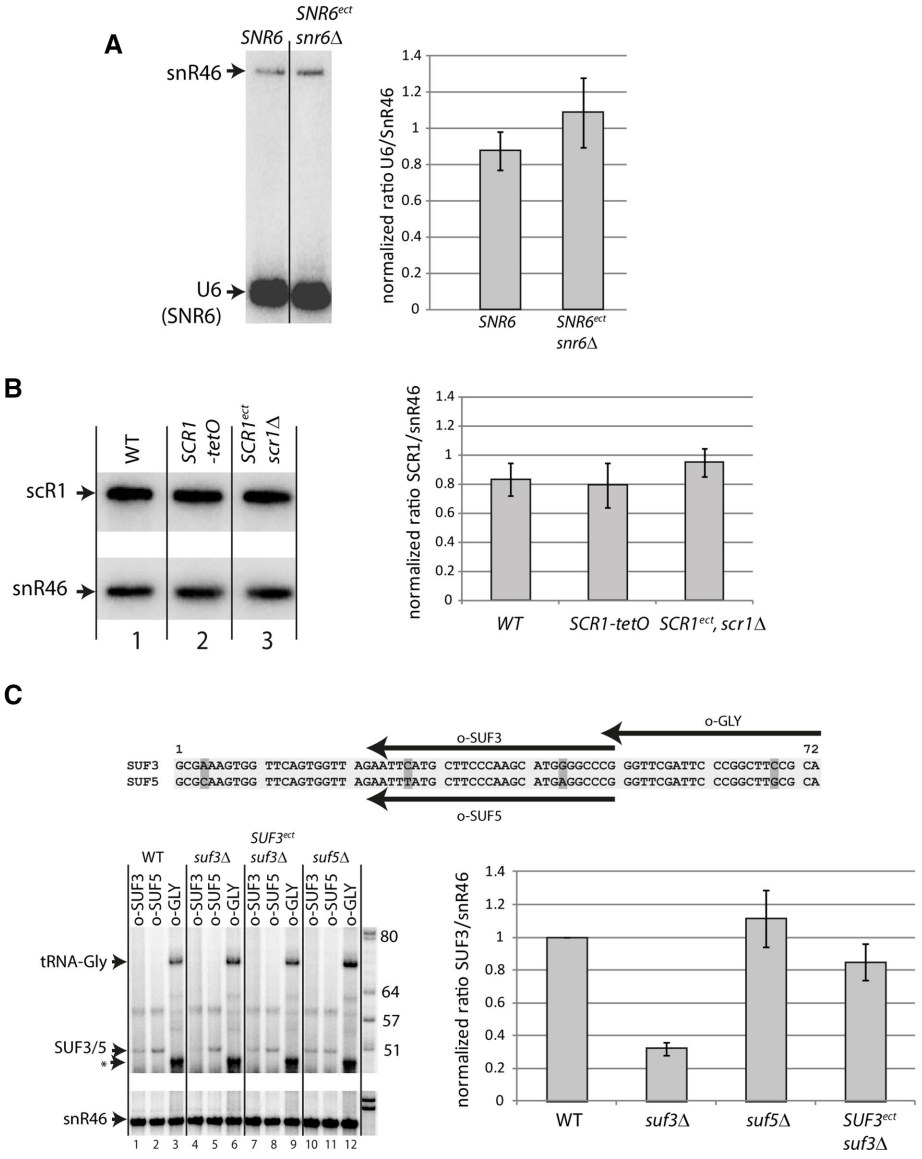

FIGURE 7: RNA accumulation from ectopically expressed Pol III–transcribed genes. (A) Quantification by northern blotting (top) of U6 transcript accumulation (bottom) relative to *SNR46* small nucleolar RNA in the wild-type strain (*SNR6*) and the strain with an ectopic *SNR6* insertion (*SNR6*^{ect}, *snr6Δ*). (B) Northern blot quantification of *SCR1* transcript accumulation relative to *SNR46* small nucleolar RNA in WT (lane1) and strains with tetO-labeled *SCR1* (lane 2) and ectopically inserted *SCR1* without a copy of *SCR1* at the native locus (*SCR1ect, scr1Δ*; lane 3). (C) Quantification by reverse transcription of *SUF3* and *SUF5* transcript accumulation relative to snR46 small nucleolar RNA (top, oligonucleotides used as primers for reverse transcription aligned with the *SUF3* and *SUF5* sequences: o-SUF3, specific to *SUF3* RNA; o-SUF5, specific to *SUF5* RNA; o-GLY was used to detect all glycine tRNAs produced from most of the tRNA^{Gly} genes). Asterisk indicates premature stop product (Figure 1).

S and G2/M phases, *SCR1* was frequently located at the nuclear periphery. tDNA docking at the nuclear envelope, exclusively in G2/M, is associated with a peak of tRNA expression during mitosis and requires Los1, the major exportin of nascent tRNA (Chen and Gartenberg, 2014). *SCR1* encodes the RNA component of the SRP particle; its location at the periphery of the nucleus during S phase may be explained by an expression pattern different from that of the tDNA.

The nucleolar and nuclear periphery regions are, therefore, preferential locations for Pol III–transcribed genes, although the locations of these genes may vary during the cell cycle.

Mechanism by which Pol III–transcribed genes associates with the nucleolus

Condensin-dependent clustering of Pol III–transcribed genes and microtubule-dependent nucleolar association of tDNAs from large families have been described (Thompson *et al.*, 2003; Haeusler *et al.*, 2008; Rodley *et al.*, 2011; Chen and Gartenberg, 2014; Rutledge *et al.*, 2015). These findings suggest that tRNA genes are involved in maintaining the spatial organization of the genome. Furthermore, chromosome conformation capture (3C) methods cluster tDNAs into two large groups: an rDNA-proximal cluster and a nonnucleolar, centromere-proximal cluster (Duan *et al.*, 2010; Rutledge *et al.*, 2015). However, some reported findings have recently been called into question. A different normalization procedure for 3C contact maps accounting for technical bias resulted in a lower estimated likelihood of Pol III–Pol III gene contacts (Cournac *et al.*, 2012). This would make a direct role for tDNA clustering in global chromosome organization less likely (Rutledge *et al.*, 2015).

By exploring individual loci by fluorescence microscopy rather than tDNA clusters by 3C-based methods, we were able to reproduce the frequent association with the nucleolar periphery of nontethered (>100 kb from *TEL*, *CEN*, and *HMR*) Pol III genes. The condensin complex is essential for the nucleolar clustering of Pol III–transcribed genes (Haeusler *et al.*, 2008). However, condensin is associated with all Pol III–transcribed genes, even those tethered away from the nucleolus (D'Ambrosio *et al.*, 2008), suggesting a role for other anchoring elements in nucleolar association. Nucleolar recruitment was abolished when Pol III transcription was inhibited. The transcripts of Pol III–transcribed genes have been reported to pass through the nucleolus during their maturation (Bertrand *et al.*, 1998). The nascent tRNAs themselves, therefore, may participate in recruiting their genes to the nucleolus. A recent study on human cells showed that Alu RNAs accumulating in the nucleolus could target other loci to the nucleolus (Caudron-Herger *et al.*, 2015). A similar mechanism in which RNA drives a DNA locus–nucleolar interaction may contribute to the association of Pol III–transcribed genes with the nucleolus in budding yeast.

Pol III–transcribed genes as a controller of local chromosome organization

Chromosome organization has been described quantitatively in yeast. Biophysical models of chromatin can be used to describe chromosomes or chromosomal rearrangements in cycling cells: the chromosomes adopt the Rabl-like configuration (Tjong *et al.*, 2012; Wong *et al.*, 2012). However, it has been suggested that other elements may tether chromosomes to the nuclear periphery (Dultz *et al.*, 2016). Our

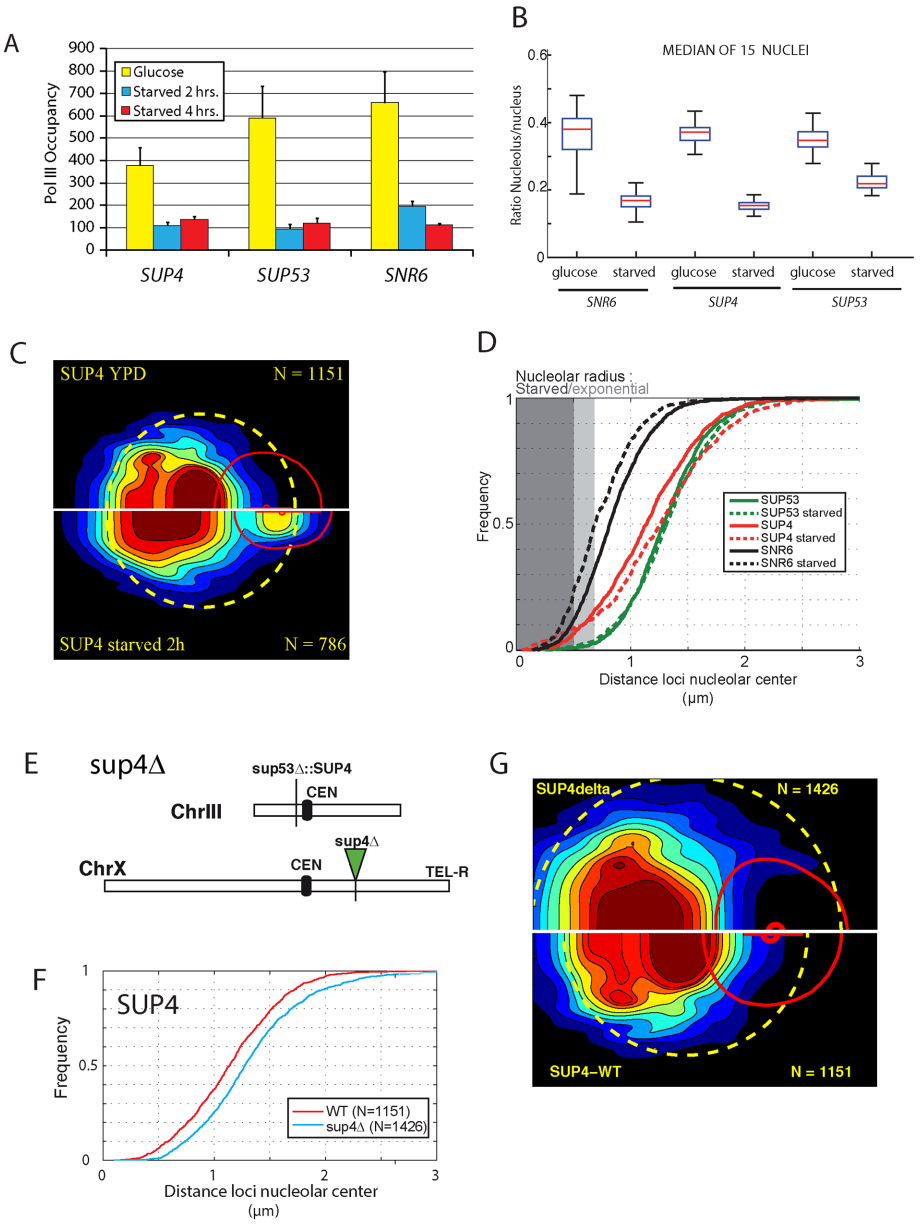

FIGURE 8: Nontethered Pol III–transcribed genes drive nucleolar periphery association. (A) Starvation results in the loss of Pol III from the genes. Pol III occupancy of genes was measured by ChIP of the 9xMyc-tagged RPC128 subunit after 2 and 4 h of starvation. Occupancy was measured by real-time PCR quantification of the loci by the *ΔΔCt* method. (B) Nucleolar/nuclear volume ratio upon nutrient depletion. Cells exponentially growing or starved of nutrients for 2 h were analyzed with NucLoc software. Boxplots of the median nucleolar-to-nuclear volume ratio (see *Materials and Methods*) were generated. (C) Gene map comparison of the position of the *SUP4* locus in exponential growth (top) and nutrient deprivation (bottom) conditions. (D) Cumulative distribution function (CDF) of the locus–nucleolar center distance (micrometers) for FROS-tagged *SUP53* (green), *SUP4* (red), and *SNR6* (black) locus. Exponential growth (solid line) and starvation conditions (dashed line). (E) FROS insertion (green triangle) near the *sup4Δ* locus on chromosome X. The gene at the *SUP4* locus was deleted and inserted into the *SUP53* locus on chromosome III. (F) CDF of locus–nucleolar center distance (micrometers) for FROS-tagged *SUP4* locus with (WT, red) and without the *SUP4* gene (*sup4Δ*, blue). (G) Gene map comparison of the *SUP4* locus (top half) with the deleted gene locus (bottom half).

findings confirm that Pol III–transcribed genes anchor the chromosomes to the nucleolus and/or NE. We demonstrate here a direct role for the nucleolus in organizing chromatin in the nucleoplasm and contributing to chromosome organization in vivo through the anchoring of Pol III–transcribed genes to its periphery.

MATERIALS AND METHODS

Yeast strains

The genotypes of the strains used are described in Supplemental Table S1. The oligonucleotides used for PCR are listed in Supplemental Table S2. We used p29802 (Berger *et al.*, 2008) as a template for PCR amplification of the KAN-MX cassette. Strains for gene mapping were constructed as previously described (Albert *et al.*, 2013). The insertion point coordinates on the chromosome and oligonucleotides used to target integration are listed in Supplemental Table S1. yCNOD15-1c, BEN56-1a, yCNOD72-1a, and yJUK03-1a were constructed by transforming the TMS1-1a strain. Strains PRA5-1a, PRA6-4a, PRA4-8a, PRA3-5a, PRA1-5a, and PRA2-7a were constructed by transforming the TMS5-8d strain.

Strains with ectopic gene insertions

We chose the *SUP53* locus for ectopic insertion because its proximity to centromere III may compete with nucleolar association, and a neighboring auxotrophic marker (*LEU2*) facilitates the desired genome modification without the need to insert an unrelated marker. Briefly, the strain construction strategy described in Supplemental Figure S2 involved construction of a receptor strain, yCNOD98-1a, in which *SUP53* and the N-terminal part of the auxotrophic selection marker *LEU2* were deleted (Supplemental Figure S2A) and a platform plasmid bearing the genomic DNA of the locus, in which *SUP53* could be replaced by any other Pol III–transcribed gene, was introduced (Supplemental Figure S2B). The targeted gene was introduced via this platform construct. Finally, two successive modifications based on homologous recombination were used to drive the ectopic insertion of a Pol III–transcribed gene at the *SUP53* locus. *LEU2*-positive clones were selected, and the native locus was invalidated in the process. The yJUK10-1a strain was generated by PCR with the 1207/1208 primers and S288c genomic DNA to restore the wild-type *LEU2* gene in the TMS1-1a strain. yCNOD98-1a was built by replacing the *SUP53* and the N-terminal part of *LEU2* in strain yJUK10-1a with a *KAN-MX* cassette, using primers 983/982. The yCNOD98-1a strain was then transformed with *Sac*I-*Hin*dIII–digested plasmids (pCNOD44, pEB5, or pBEL7) to generate ectopic insertions of *SNR6*, *SUF3*, and *SCR1* (PRA14-1a), respectively. The extra copy at the wild-type locus was removed by inserting the *KAN-MX* cassette with primer pairs 1254/1255 (*SNR6*), 1286/1287 (*SUF3*), and 1298/1299 (*SCR1*) to generate strains BEL1-6a, PRA13-1a, and PRA15-2a, respectively. *SUF3* and *SUF5* were deleted in strain yJUK10-1a with primers

1286/1287 and 1292/1293 to generate BEL5-1a and BEL6-7a, respectively. TetO insertions were performed, as described for strain yJUK03-1a, in strains BEL1-6a, PRA13-1a, and PRA15-2a to generate strains BEL4-2a, PRA8-1a, and PRA11-1a, respectively.

Deletion strains

SUF5 was deleted from PRA2-7a by transformation with an integrative URA3 PCR fragment amplified with primers 1292/1293 from pSK-URA3-M13 used as a template. This deletion generated the yCNOD165-1a strain. yCNOD178-1a and yCNOD142-1a, carrying labeled deletions of *SUF3* and *SCR1*, respectively, were obtained by *his3Δ-tetO-NAT* insertion into the ectopic strains PRA13-1a (*SUF3ect*) and PRA15-2a (*SCR1ect*). The labeling strategies were identical to those used when generating strains PRA1-5a (*SUF3*) and PRA3_5a (*SCR1*). We deleted *TRT2*, *TRR4*, and *SUP4*, by introducing the *(sup53Δ-leu2ΔNter)::KAN-MX* cassette used for ectopic insertion into strains with labeled loci by mating PRA5-1a (*TRT2*) and PRA4-8a (*TRR4*) with yCNOD98-1a, and yCNOD72-1a (*SUP4*) with yCNOD148-7b, and then allowing sporylation to occur. Selected spores were transformed with *Sac*I/*Hin*dIII–digested pCNOD60 (*TRT2*), pCNOD58 (*TRR4*), or pCNOD45 (*SUP4*) to insert ectopic copies. The WT gene copies were deleted by transformation with URA3 amplified from pSK-URA3-M13 by integrative PCR with the primer pairs 1480/1481 (*TRT2*), 1302/1470 (*TRR4*), and 1256/1257 (*SUP4*). This generated strains yCNOD166-1a (*TRT2*), yCNOD163-1a (*TRR4*), and yCNOD190-2a (*SUP4*), respectively, carrying labeled deletions.

Ectopic rDNA at CEN5

Strain rDNA-CEN5 (yCNOD191-1a) was constructed as follows. MATalpha strain NOY2030 carrying rDNA at CEN5 (Oakes *et al.*, 2006) was converted into MATa, and spontaneous *URA3*$^+$ revertants were isolated. They were then mated with strain TMS5-8d, which is suitable for use for gene labeling. After meiosis, yCNOD130-4b spores carrying rDNA at CEN5 (checked by pulsed-field gel electrophoresis) and suitable markers were selected. These spores lacked the *TetR-GFP* gene, which was subsequently reintroduced in two steps. First, a large 3′ deletion (*lys2Δ::KAN*) was introduced into the *LYS2* gene (primers 1497/1498, template p29802). In the second step, a *Bgl*II-linearized *TetR-GFP* (pE219) plasmid was inserted into the *lys2Δ::KAN* allele. *SNR6* or *SUP53* was labeled in yCNOD191-1a, as described for yJUK03-1a and yCNOD15-1c. This labeling resulted in the strains yCNOD182-1a (*SNR6*) and yCNOD184-1a (*SUP53*). The centromere was labeled with *SPC42-CFP* in strain yCNOD130-4b (rDNA-CEN5), generating strains yCNOD186-1a and TMS1-1a (control), giving rise to yCNOD192-1a. A *CFP-KAN* PCR fragment was amplified by integrative PCR from pDH3 (pFA6-CFP-KAN) with oligonucleotides 1492 and 1493.

Conditional centromere

Strain yCNOD171-1a (pGAL-CEN3) is a derivative of strain yJUK03-1a. We inserted pGAL at *CEN3*, using pCEN03-UG (Reid *et al.*, 2008) according to the authors' protocol. The control strain pGAL-CEN9 (yCNOD174-1a) was generated like yCNOD171-1a but with pCEN09-UG. We generated yCNOD173-1a (cen3Δ-CEN6) by inserting the *Nco*I-linearized centromeric plasmid pCNOD69 into yCNOD171-1a at the *YCR101c* locus. Integration events were selected on SC-galactose minus leucine plates, leading to the selection of strain yCNOD172-1a. The pGAL-CEN3 conditional centromere was then fully deleted with a *KAN-MX* PCR fragment amplified with primers 1507/1508 and plasmid p29802. Transformants were selected on glucose-containing medium.

Plasmid construction

The plasmids used in this study are listed in Supplemental Table S3. For ectopic insertion, plasmids were constructed as follows. First, a PCR fragment containing *SUP53* and the N-terminal part of *LEU2* was amplified with the 1220/1219 primers from S288c genomic DNA and inserted as a *Sac*I/*Hin*dIII fragment into pUC19 to generate pCNOD40. pCNOD41, carrying *SUP53* flanked by *Xho*I and *Bam*HI sites, was then generated by site-directed mutagenesis of pCNOD40 with primers 980 and 981. *SUP4, TRR4, TRT2, SNR6, SUF3*, and *SCR1* were amplified from S288c genomic DNA by PCR with primer pairs 1221/1222, 1312/1313, 1486/1487, 1223/1224, 1304/1305, and 1347/1311, respectively. PCR fragments were inserted into pCNOD41 as *Xho*I/*Bam*HI fragments in place of *SUP53* to generate pCNOD45 (*SUP4*), pCNOD58 (*TRR4*), pCNOD60 (*TRT2*), pCNOD44 (*SNR6*), pBEL5 (*SUF3*), and pBEL7 (*SCR1*). A similar strategy was used to insert *RDN5* into pBEL8, except that pNOY373 was used as the template for PCR with primers 1308/1309. The integrative plasmid pCNOD69 was constructed by amplifying the *YCR101c* locus from S288c genomic DNA with primers 1494/1495 and inserting the resulting *Hin*dIII/*Bam*HI–digested fragment inserted into the vector pRS315.

Fluorescence microscopy of living yeast cells

Cell culture. Yeast media were used as previously described (Rose *et al.*, 1990). YPD consists of 1% yeast extract, 2% peptone, and 2% dextrose. SC consists of 0.67% nitrogen base without amino acids (BD Difco, Franklin Lakes, NJ) and 2% dextrose supplemented with amino acid mixture (AA mixture; Bio101, Carlsbad, CA), adenine, and uracil. Cells were grown overnight at 30°C in YPD diluted to 10^6 cells/ml, harvested at a density of 4×10^6 cells/ml, and rinsed twice with the corresponding SC medium. Cells were spread on slides coated with a patch of SC medium supplemented with 2% agarose and 2% glucose. Cover slides were sealed with VaLaP (one-third Vaseline, one-third lanolin, one-third paraffin). For starvation experiments, cell cultures reaching a density of 4×10^6 cells/ml were washed twice with 15% YP without glucose, resuspended at a density of 4×10^6 cells/ml in this medium, and incubated for 2 h at 30°C. Cells were mounted on slides as described but with 15% SC without glucose.

Microscope image acquisition. *Gene position*. Confocal microscopy was performed within 20 min of mounting, using an Andor Revolution Nipkow-disk confocal system (Andor Technology, Bellfast, Northern Ireland) installed on an Olympus IX-81 (Olympus Corporation, Tokyo, Japan), featuring a CSU22 confocal spinning-disk unit (Yokogawa, Tokyo, Japan) and an electron-multiplying charge-coupled device camera (DU 888; Andor). The system was controlled with the Revolution FAST mode of Andor Revolution IQ1 software. Images were acquired with an Olympus 100× objective (Plan APO, 1.4 numerical aperture [NA], oil immersion). The single laser lines used for excitation were from diode-pumped solid-state lasers exciting GFP fluorescence at 488 nm (50 mW; Coherent, Santa Clara, CA) and mCherry fluorescence at 561 nm (50 mW; CoboltJive; Cobolt AB, Solna, Sweden). A Semrock (Rochester, NY) bi-bandpass emission filter (Em01-R488/568-15) was used to collect green and red fluorescence. Pixel size was 65 nm. For 3D analysis, *Z*-stacks of 41 images with a 250-nm *Z*-step were used. An exposure time of 200 ms was applied.

SPB imaging. Fluorescence imaging was performed with an Olympus inverted microscope equipped with a complementary metal-oxide semiconductor camera (Hamamatsu ORCA-Flash 4.0;

Hamamatsu, Hamamatsu City, Japan) and a SpectraX illumination system (Lumencore, Beaverton, OR). Images were acquired with an Olympus UPlan SApo 100× objective lens (NA 1.4) and a dual-band cyan fluorescent protein (CFP)–yellow fluorescent protein Semrock filter set (excitation, 416/501-25; DM440/520-Di01-25×36; emission, 464/547-25) for CFP and a three-band Chroma (Bellows Falls, VT) filter set (69002 ET-DAPI/FITC/Texas Red) in combination with an eternal filter wheel equipped with Semrock filters with emission 465/537/623 and 520-40 for mCherry and GFP, respectively.

Image analysis to determine locus position. Confocal images were processed and analyzed with a Matlab (The MathWorks, Natick, MA) script, NucLoc, available from www.nucloc.org (Berger *et al.*, 2008). Cumulative distribution functions were generated with an existing function (Matlab). Boxplots of median ratios of distances to the center of the nucleolus or nucleus were generated in two steps by first calculating median distances for each of 100 nuclei and then plotting boxplots for the median values obtained.

RNA analysis

The sequences of the oligonucleotides used for RNA quantification are given in Supplemental Table S3. RNA was extracted and Northern blotting performed as previously described (Beltrame and Tollervey, 1992). Reverse transcription was performed with the Superscript II kit (Invitrogen, Carlsbad, CA) in accordance with the manufacturer's protocol. RNA species were resolved by electrophoresis on 8% polyacrylamide sequencing gels. Quantifications were performed by phosphorimaging (Typhoon; GE Healthcare, Little Chalfont, UK) with MultiGauge software (Fujifilm, Tokyo, Japan).

Chromatin immunoprecipitation

The YPH500 RPC128-myc strain was grown to mid exponential growth phase ($OD_{600\ nm}$ = 0.8) and cross-linked by incubation with 1% formaldehyde for 30 min. ChIP samples were prepared as previously described (Arimbasseri and Bhargava, 2008; Mahapatra *et al.*, 2011; Kumar and Bhargava, 2013) with an anti-Myc antibody (05-724; Merck Millipore, Darmstadt, Germany). Real-time PCR was performed on the ChIP and control (input and no antibody) DNA to determine Pol III occupancy on *SNR6* (primers 1 and 2), *SUP4* (primers 3 and 4), and *SUP53* (primers 5 and 6) genes. Pol III occupancy was normalized relative to that on *TelVIR* (primers 7 and 8) used as a negative control and is expressed as fold enrichment relative to the negative control.

Mononucleosome MNase protection assay

Untagged control (TMS5-8a) and FROS insertion (for genes *TRT2*, *TRR4*, *SUF3*, *SUF5*, and *SUP61*) strains were grown to mid exponential growth phase (OD = 0.8) at 30°C. Cells were cross-linked by incubation with 1% formaldehyde for 10 min, and the reaction was quenched by adding 125 mM glycine. Cells were washed, and spheroplasts were generated with Zymolyase (AMS Biotechnology, Abingdon, UK). Spheroplasts were subjected to controlled MNase digestion, and the digested DNA was purified and subjected to electrophoresis in 1.25% agarose gels. Naked genomic DNA (deproteinized) was digested with MNase to obtain a fragment distribution ranging from 100 to 300 base pairs for use as a control. The band corresponding to mononucleosomal DNA was excised from the gel, and the DNA was purified. Equal amounts of mononucleosomal DNA and digested genomic DNA were used as a template for real-time PCR. Nucleosome occupancy was investigated with primers designed to amplify 110 ± 10–base pair fragments close to the tDNA gene. Nucleosome occupancy was normalized relative to a control subtelomeric region of TelVIR.

ACKNOWLEDGMENTS

We thank Juliane Klehr for strain construction and initial characterization of the positions of loci. This work also benefited from the assistance of the imaging platform of Toulouse (Toulouse Reseau Imagerie). This work was supported by an ATIP-plus grant from the Centre National de la Recherche Scientifique, the Agence Nationale de la Recherche (ANDY), and the IDEX of Toulouse University (Clemgene and Nudgene). This work is a French–Indian collaborative effort funded by Indo-French Centre for the Promotion of Advanced Research Project 4103 between the laboratories of P.B. and O.G.

REFERENCES

Albert B, Mathon J, Shukla A, Saad H, Normand C, Leger-Silvestre I, Villa D, Kamgoue A, Mozziconacci J, Wong H, *et al.* (2013). Systematic characterization of the conformation and dynamics of budding yeast chromosome XII. J Cell Biol 202, 201–210.

Arimbasseri AG, Bhargava P (2008). Chromatin structure and expression of a gene transcribed by RNA polymerase III are independent of H2A.Z deposition. Mol Cell Biol 28, 2598–2607.

Beltrame M, Tollervey D (1992). Identification and functional analysis of two U3 binding sites on yeast pre-ribosomal RNA. EMBO J 11, 1531–1542.

Berger AB, Cabal GG, Fabre E, Duong T, Buc H, Nehrbass U, Olivo-Marin JC, Gadal O, Zimmer C (2008). High-resolution statistical mapping reveals gene territories in live yeast. Nat Methods 5, 1031–1037.

Bertrand E, Houser-Scott F, Kendall A, Singer RH, Engelke DR (1998). Nucleolar localization of early tRNA processing. Genes Dev 12, 2463–2468.

Bloom-Ackermann Z, Navon S, Gingold H, Towers R, Pilpel Y, Dahan O (2014). A comprehensive tRNA deletion library unravels the genetic architecture of the tRNA pool. PLoS Genet 10, e1004084.

Bystricky K, Laroche T, van Houwe G, Blaszczyk M, Gasser SM (2005). Chromosome looping in yeast: telomere pairing and coordinated movement reflect anchoring efficiency and territorial organization. J Cell Biol 168, 375–387.

Casolari JM, Brown CR, Komili S, West J, Hieronymus H, Silver PA (2004). Genome-wide localization of the nuclear transport machinery couples transcriptional status and nuclear organization. Cell 117, 427–439.

Caudron-Herger M, Pankert T, Seiler J, Nemeth A, Voit R, Grummt I, Rippe K (2015). Alu element-containing RNAs maintain nucleolar structure and function. EMBO J 34, 2758–2774.

Chen M, Gartenberg MR (2014). Coordination of tRNA transcription with export at nuclear pore complexes in budding yeast. Genes Dev 28, 959–970.

Cournac A, Marie-Nelly H, Marbouty M, Koszul R, Mozziconacci J (2012). Normalization of a chromosomal contact map. BMC Genomics 13, 436.

D'Ambrosio C, Schmidt CK, Katou Y, Kelly G, Itoh T, Shirahige K, Uhlmann F (2008). Identification of cis-acting sites for condensin loading onto budding yeast chromosomes. Genes Dev 22, 2215–2227.

Duan Z, Andronescu M, Schutz K, McIlwain S, Kim YJ, Lee C, Shendure J, Fields S, Blau CA, Noble WS (2010). A three-dimensional model of the yeast genome. Nature 465, 363–367.

Dultz E, Tjong H, Weider E, Herzog M, Young B, Brune C, Mullner D, Loewen C, Alber F, Weis K (2016). Global reorganization of budding yeast chromosome conformation in different physiological conditions. J Cell Biol 212, 321–334.

Gehlen LR, Gruenert G, Jones MB, Rodley CD, Langowski J, O'Sullivan JM (2012). Chromosome positioning and the clustering of functionally related loci in yeast is driven by chromosomal interactions. Nucleus 3, 370–383.

Gong K, Tjong H, Zhou XJ, Alber F (2015). Comparative 3D genome structure analysis of the fission and the budding yeast. PLoS One 10, e0119672.

Gotta M, Laroche T, Formenton A, Maillet L, Scherthan H, Gasser SM (1996). The clustering of telomeres and colocalization with Rap1, Sir3, and Sir4 proteins in wild-type Saccharomyces cerevisiae. J Cell Biol 134, 1349–1363.

Gursoy G, Xu Y, Liang J (2014). Computational predictions of structures of multichromosomes of budding yeast. Conf Proc IEEE Eng Med Biol Soc 2014, 3945–3948.

Haeusler RA, Engelke DR (2004). Genome organization in three dimensions: thinking outside the line. Cell Cycle 3, 273–275.

Haeusler RA, Engelke DR (2006). Spatial organization of transcription by RNA polymerase III. Nucleic Acids Res 34, 4826–4836.

Haeusler RA, Pratt-Hyatt M, Good PD, Gipson TA, Engelke DR (2008). Clustering of yeast tRNA genes is mediated by specific association of condensin with tRNA gene transcription complexes. Genes Dev 22, 2204–2214.
Hernandez-Verdun D, Roussel P, Gebrane-Younes J (2002). Emerging concepts of nucleolar assembly. J. Cell Sci 115, 2265–2270.
Hill A, Bloom K (1987). Genetic manipulation of centromere function. Mol Cell Biol 7, 2397–2405.
Jakociunas T, Domange Jordo M, Ait Mebarek M, Bunner CM, Verhein-Hansen J, Oddershede LB, Thon G (2013). Subnuclear relocalization and silencing of a chromosomal region by an ectopic ribosomal DNA repeat. Proc Natl Acad Sci USA 110, E4465–E4473.
Jin QW, Fuchs J, Loidl J (2000). Centromere clustering is a major determinant of yeast interphase nuclear organization. J Cell Sci 113, 1903–1912.
Klein F, Laroche T, Cardenas ME, Hofmann JF, Schweizer D, Gasser SM (1992). Localization of RAP1 and topoisomerase II in nuclei and meiotic chromosomes of yeast. J Cell Biol 117, 935–948.
Kumar Y, Bhargava P (2013). A unique nucleosome arrangement, maintained actively by chromatin remodelers facilitates transcription of yeast tRNA genes. BMC Genomics 14, 402.
Léger-Silvestre I, Trumtel S, Noaillac-Depeyre J, Gas N (1999). Functional compartmentalization of the nucleus in the budding yeast Saccharomyces cerevisiae. Chromosoma 108, 103–113.
Mahapatra S, Dewari PS, Bhardwaj A, Bhargava P (2011). Yeast H2A.Z, FACT complex and RSC regulate transcription of tRNA gene through differential dynamics of flanking nucleosomes. Nucleic Acids Res 39, 4023–4034.
Misteli T (2001). The concept of self-organization in cellular architecture. J Cell Biol 155, 181–185.
Misteli T (2007). Beyond the sequence: cellular organization of genome function. Cell 128, 787–800.
Nemeth A, Conesa A, Santoyo-Lopez J, Medina I, Montaner D, Peterfia B, Solovei I, Cremer T, Dopazo J, Langst G (2010). Initial genomics of the human nucleolus. PLoS Genet 6, e1000889.
Oakes ML, Johzuka K, Vu L, Eliason K, Nomura M (2006). Expression of rRNA genes and nucleolus formation at ectopic chromosomal sites in the yeast Saccharomyces cerevisiae. Mol Cell Biol 26, 6223–6238.
Reid RJ, Sunjevaric I, Voth WP, Ciccone S, Du W, Olsen AE, Stillman DJ, Rothstein R (2008). Chromosome-scale genetic mapping using a set of 16 conditionally stable Saccharomyces cerevisiae chromosomes. Genetics 180, 1799–1808.
Roberts DN, Stewart AJ, Huff JT, Cairns BR (2003). The RNA polymerase III transcriptome revealed by genome-wide localization and activity-occupancy relationships. Proc Natl Acad Sci USA 100, 14695–14700.
Rodley CD, Pai DA, Mills TA, Engelke DR, O'Sullivan JM (2011). tRNA gene identity affects nuclear positioning. PLoS One 6, e29267.
Rose MD, Winston F, Hieter P (1990). Methods in Yeast Genetics. A Laboratory Manual, Cold Spring Harbor, NY: Cold Spring Harbor Laboratory Press.
Rutledge MT, Russo M, Belton JM, Dekker J, Broach JR (2015). The yeast genome undergoes significant topological reorganization in quiescence. Nucleic Acids Res 43, 8299–8313.
Takizawa T, Meaburn KJ, Misteli T (2008). The meaning of gene positioning. Cell 135, 9–13.
Therizols P, Duong T, Dujon B, Zimmer C, Fabre E (2010). Chromosome arm length and nuclear constraint determine the dynamic relationship of yeast subtelomeres. Proc Natl Acad Sci USA 107, 2025–2030.
Thompson M, Haeusler RA, Good PD, Engelke DR (2003). Nucleolar clustering of dispersed tRNA genes. Science 302, 1399–1401.
Tjong H, Gong K, Chen L, Alber F (2012). Physical tethering and volume exclusion determine higher-order genome organization in budding yeast. Genome Res 22, 1295–1305.
Tokuda N, Terada TP, Sasai M (2012). Dynamical modeling of three-dimensional genome organization in interphase budding yeast. Biophys J 102, 296–304.
Trumtel S, Leger-Silvestre I, Gleizes PE, Teulieres F, Gas N (2000). Assembly and functional organization of the nucleolus: ultrastructural analysis of Saccharomyces cerevisiae mutants. Mol Biol Cell 11, 2175–2189.
Verdaasdonk JS, Vasquez PA, Barry RM, Barry T, Goodwin S, Forest MG, Bloom K (2013). Centromere tethering confines chromosome domains. Mol Cell 52, 819–831.
Wong H, Marie-Nelly H, Herbert S, Carrivain P, Blanc H, Koszul R, Fabre E, Zimmer C (2012). A predictive computational model of the dynamic 3D interphase yeast nucleus. Curr Biol 22, 1881–1890.
Yang CH, Lambie EJ, Hardin J, Craft J, Snyder M (1989). Higher order structure is present in the yeast nucleus: autoantibody probes demonstrate that the nucleolus lies opposite the spindle pole body. Chromosoma 98, 123–128.
Zimmer C, Fabre E (2011). Principles of chromosomal organization: lessons from yeast. J Cell Biol 192, 723–733.